A PRELIMINARY STRUCTURAL ANALYSIS OF THE TOROIDAL FIELD COILS FOR T-10M*

W. H. Gray and J. K. Ballou
Fusion Energy Division

W.C.T. Stoddart
Engineering Division

Oak Ridge National Laboratory
Oak Ridge, Tennessee 37830

G. F. Churakov
Efremov Institute, Leningrad, U.S.S.R.

E. Y. Klimenko
Kurchatov Institute, Moscow, U.S.S.R.

Paper to be presented at the Seventh Symposium on Engineering Problems of Fusion Research, Hyatt Regency, Knoxville, Tennessee, October 24-28, 1977

*Research sponsored by the Department of Energy under contract with Union Carbide Corporation.

A PRELIMINARY STRUCTURAL ANALYSIS OF THE TOROIDAL FIELD COILS FOR T-10M*

W. H. Gray and J. K. Ballou
Fusion Energy Division

W.C.T. Stoddart
Engineering Division

Oak Ridge National Laboratory
Oak Ridge, Tennessee 37830

G. F. Churakov
Efremov Institute, Leningrad, U.S.S.R.

E. Y. Klimenko
Kurchatov Institute, Moscow, U.S.S.R.

Abstract

A structural analysis of the T-10M tokamak toroidal field (TF) coil system has been performed. Two TF coil shapes were proposed, one oval and the other circular. Each TF coil system is composed of 24 coils. The oval TF coil system has a 2.4-m major radius with a minor bore diameter of 2.15 m and a major bore diameter of 3.28 m. The circular TF coil system has a 2.5-m major radius with a 2.2-m bore diameter. The cross sections of both TF coil shapes have rectangular dimensions of 0.4 m by 0.26 m with a 0.36-m by 0.22-m winding cavity symmetrically placed within the cross section. The current of each coil is 1.75 MA. Either geometry produces a magnetic field of 3.5 T on axis, 2.4 m from the machine center line.

This study reports the results of a cooperative investigation to determine which TF coil shape operates in a minimum stress configuration. The study is a part of the joint U.S.A./U.S.S.R. scientific exchange. The scope of the analysis covers only the in-plane force distribution produced by the magnetic field.

Based upon the preceding conditions the oval TF coil shape appears to be superior to the circular TF coil shape. Further, the oval TF coil shape in its present design has a significant safety margin between working and yield stress under normal operating conditions. The circular design, however, is less sensitive to magnetic field perturbations which may be encountered in proof testing.

Introduction

A structural analysis of the T-10M tokamak toroidal field (TF) coil system was performed. Two TF coil shapes were proposed, one oval and the other circular. Each TF coil system consisted of 24 coils. The circular TF coil system has a 2.5-m major radius with a 2.2-m bore diameter coil. The oval TF coil system has a 2.4-m major radius with a minor bore diameter of 2.15 m and a major bore diameter of 3.28 m. The oval shape was generated by four circular arcs (see *Fig. 1*), and therefore represents a compromise between the fabrication difficulties associated with a continuously varying radius of curvature and the constant tension characteristics obtainable in approximately D-shaped coils.

Both TF coil shape cross sections had the rectangular dimensions of 0.4 m by 0.26 m with a 0.36-m by 0.22-m winding cavity symmetrically placed within the cross section. The current was 1.75 MA. Figure 2 presents a three-dimensional plot of the 24 coils which make up the oval TF coil array. The coils were divided into four circular arcs to make a geometrical description for a magnetic field code. This geometry produced a magnetic field of 3.5 T on axis, 2.4 m from the machine center line of each tokamak. For the representation in Fig. 2 each circular arc was again divided into four sections and approximated with planar panels. This geometrical description was processed by a hidden line removal graphics package to produce Fig. 2.

The objective of this study was to determine which one of the TF coil shapes was the "best" design; that is, which one operated in a minimum stress configuration. The scope of the analysis covered only the in-plane force distribution produced by the magnetic field. Thermal, gravity, and conductor pretensioning loads were neglected since coil shape considerations are less sensitive to these factors. Further, out-of-plane magnetic loading as well as out-of-plane support schemes were not examined.

Electromagnetic Force Calculation

Two in-plane electromagnetic force distributions were analyzed for each coil. The first was due to normal dc operation of the TF coils arranged in a toroidal array. The second was a perturbation of the first which varied from an increase of 0% at the location of the maximum force to an increase of 30% at the location of the minimum force, thereby simulating a proof test of a coil in an externally generated background magnetic field.

The calculation of the normal electromagnetic force was performed using the simplified force per unit length formula derived in[1]

$$f_\ell = \frac{\mu_0 N I^2}{4\pi R}\left[1 + \frac{1}{N}\left(\cos\theta + \frac{R}{\rho}\ln\frac{1.284R}{CN}\right)\right] \qquad (1)$$

where f_ℓ is the force per unit length, N is the number of coils, I is the current, R is the toroidal radius to the point in question, ρ is the radius of curvature at this point, C is the cross-sectional radius of the conductor, and θ is the angle the radius of curvature vector makes with the horizontal axis.

For the circular coil, application of Eq. (1) was straightforward. However, the present design of the oval coil leads to application problems with Eq. (1). Because the proposed coil is not tangent at the arc intersection locations, discontinuities arise in the radius of curvature and in the f_ℓ calculated by Eq. (1). Due to lack of time to devote to these calculations, the resulting f_ℓ calculation simply averaged the f_ℓ values at each side of a discontinuity.

Stress Analysis Models

For each TF coil shape and loading case two finite element models were analyzed. The first and more conservative model considered the coil case to be the only supporting member of the coil cross section. Eighteen hollow rectangular beams were used to describe the TF coil geometry from a point where the TF coil would be supported by contacting the machine bucking cylinder to the plane of symmetry of the coil, approximately 120° away (Fig. 3).

*Research sponsored by the Department of Energy under contract with Union Carbide Corporation.

The second model like the first included 18 hollow rectangular beam elements; however, it also had 18 rectangular rod elements modeling the stretching resistance of the monolithic conductor cross section without introducing any bending stiffness for the conductor.

The material used for the case was stainless steel with a Young's Modulus of 193 GPa (~30 x 10^6 psi) and a design stress of 276 MPa (~40 ksi). The material properties assumed for the conductor were that of copper reduced by 0.74 to account for helium channels which surround each conductor element. The reduced conductor Young's Modulus and design stress were 36.7 GPa and 103 MPa, respectively.

The previously calculated loads were introduced into the finite element models using linear interpolation at those node points where forces were not calculated. The GIFTS IV[2] computer code was used for the model generation as well as solution.

Results

Output of interest from the finite element models consisted of stresses at the inner and outer fibers of the beam elements and deflections of all the node points. An example of the output from GIFTS IV is shown in Fig. 4. This figure depicts the distribution of the bending stresses on beam element 2 of model DT10, loading case 1. This is the oval coil model with rod elements stressed by the normal operational load. Such figures were made for all of the beam elements in every model. These data were condensed into the following eight figures.

In the next eight figures normal stress in the coil case is plotted versus angular position around the TF coil (an angle of 180° is located at the point on the coil furthest from the machine centerline). The plots show four values of stress: the outer fiber stress, the inner fiber stress, the membrane stress, and the bending stress. The outer and inner fiber stresses occur at the outer and inner surfaces of a coil (Fig. 1). Values of stress are graphed in percent of the design stress for stainless steel which is 276 MPa. The outer and inner fiber stresses are those which are actually predicted to occur at their respective locations. The membrane stress is the average of the inner and outer stress and represents the amount of the force which is being resisted in tension. The bending stress is the average difference between the inner and outer stress and represents the amount of force which is being resisted in bending. On the graphs which follow, it is shown that small values of bending stress relative to the magnitudes of the other stresses are desirable.

Figure 5 presents stress versus angular position for the oval coil model with the case being considered as the only structural member resisting the electromechanical force. This response is due to the normal force distribution. The graph demonstrates that the oval coil is relatively bending free, as only 20-25% of its stress is due to bending relative to its membrane stress. Figure 6 shows the stress response of the same model as Fig. 5 except the perturbed force distribution was used in the analysis. Comparison of this figure with Fig. 5 demonstrates that the oval coil shape is very sensitive to force distributions which may be induced during a proof test. Unlike the previous figure, 30-35% of its stress is due to bending rather than membrane stress.

Figures 7 and 8 present the circular coil geometry instead of the oval coil geometry; first with the normal force distribution and next with the perturbed force distribution. Both models, like the two previous ones, have only beam elements restraining the electromechanical forces. Comparison of the circular model in Fig. 7 with the oval model in Fig. 5 shows significantly more bending in the circular model, as one would expect. However, when the perturbed force distribution is acting upon the circular model (Fig. 8), the stress levels are relatively unchanged compared to the normal force distribution in Fig. 7. The perturbed force condition is more nearly the bending free pattern for a circular coil shape. This fact is one of the fundamental differences in response to load between the two coil geometries.

Figures 9-12 correspond directly to Figs. 5-8, except that each of these plots was obtained by assuming the conductor would offer some degree of stretching resistance to load without any bending resistance. Figures 9-12 generally show the same trends as their counterparts, but the magnitudes of the inner and outer fiber stresses are lower.

Conclusions

Table 1 presents a summary of the differences between the structural response of the oval and circular TF coil models for both in-plane magnetic force distributions. The following results were obtained from the stress analysis.

(1) The circular TF coil has 50% higher stress than the oval TF coil for normal force distributions.

(2) The oval coil is relatively bending free in the normal force field, as only 20-25% of its stress is due to bending.

(3) The circular coil peak stress was insensitive to the force distribution perturbations whereas the oval coil stress was very sensitive.

(4) The addition of the tension-only conductor elements (model 2) decreased the stresses in both coil shapes by approximately 25%.

Based upon these results the oval TF coil shape appears to be superior to the circular TF coil shape. Further, the oval TF coil shape in its present design has a significant safety margin between working and yield stress under normal operating conditions.

References

1. Moses, R. W., Jr., and Young, W. C., Proc. 6th Symposium on Engineering Problems of Fusion Research, IEEE Pub. No. 75CH1097-5-NPS.

2. Kamel, H. A. and McCabe, M. W., "GIFTS IV Users Manual," University of Arizona, Tucson, Arizona, 1976.

Table 1. A comparison of the maximum predicted stress* for each TF coil shape, force field, and model for the T-10M Tokamak

Oval Stress / Circular Stress	Force 1 (Normal)	Force 2 (Perturbed)
Model 1 case only	67% 93%	97% 92%
Model 2 case and conductor	50% 76%	77% 71%

*The percentages listed are of the design stress of 276 MPa (~40 ksi).

ORNL/DWG/FED-77307

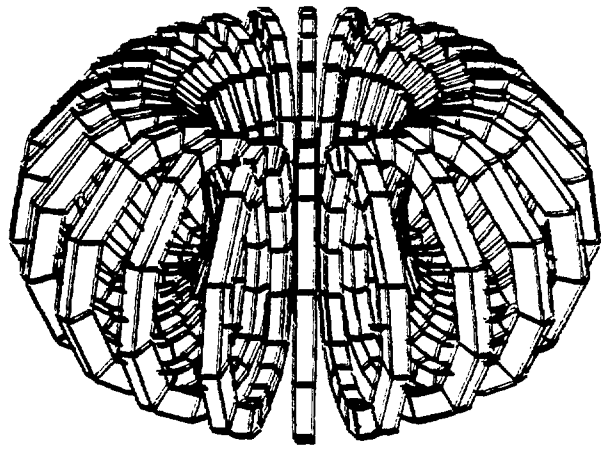

Fig. 2. Three-dimensional plot of the geometrical representation of the TF coils for tokamak T-10M. Data for this graph were obtained directly from the geometrical data base used by a magnetic field code to calculate field. For the purpose of presentation the hidden lines have been removed from this drawing.

ORNL/DWG/FED-77683

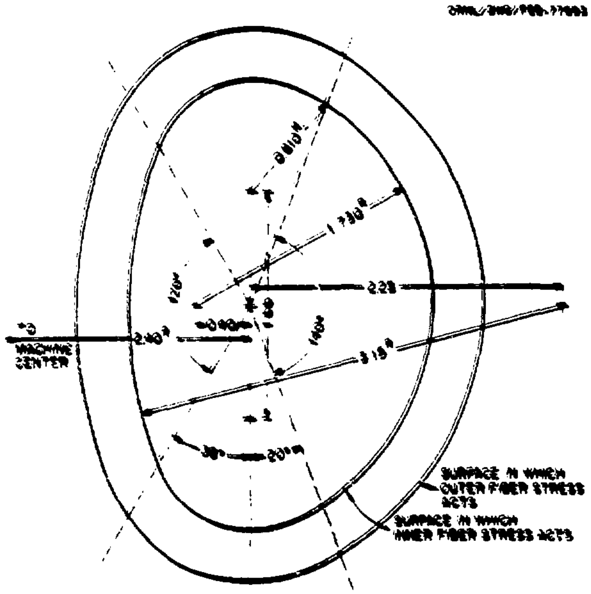

Fig. 1. Oval coil concept for the T-10M tokamak toroidal field coil system.

ORNL/DWG/FED-77769

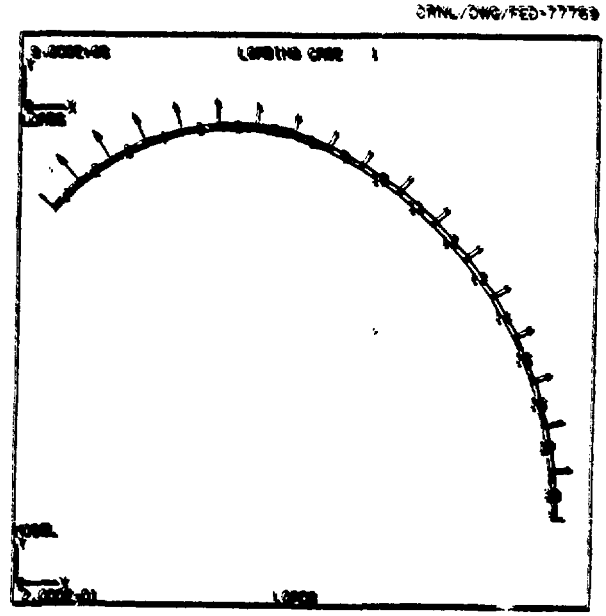

Fig. 3. Graph of the 18 hollow rectangular beam elements used to geometrically describe the oval T-10M TF coil concept. Note that half symmetry was used to decrease model size and that the backing cylinder was considered to be infinitely rigid.

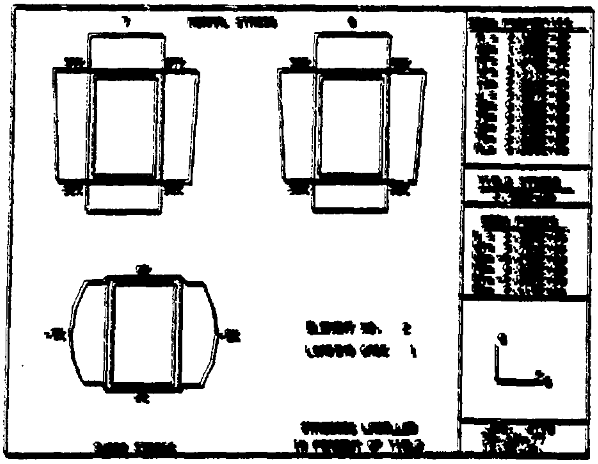

Fig. 4. Example output from the GIFTS IV computer code. At node 7 (the left end of the beam element 2), the normal stress varies from 37% of yield stress at the outer beam surface to 32% of yield stress at the inner beam surface. At node 8 (the right end of beam element 2), the normal stress varies from 38% of yield stress at the outer beam surface to 37% of yield stress at the inner beam surface. A yield stress of 276 MPa (~40 ksi) was used in the analysis. This beam element is carrying the majority of its load in tension.

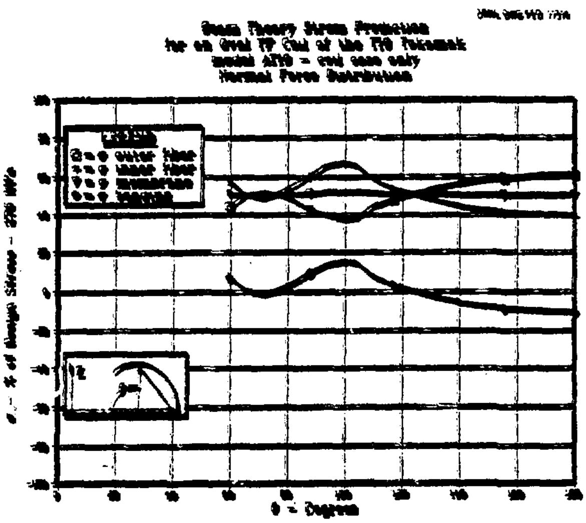

Figure 5.

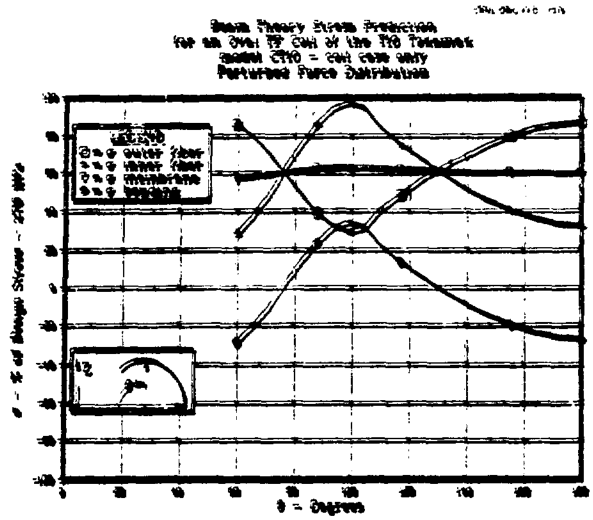

Figure 6.

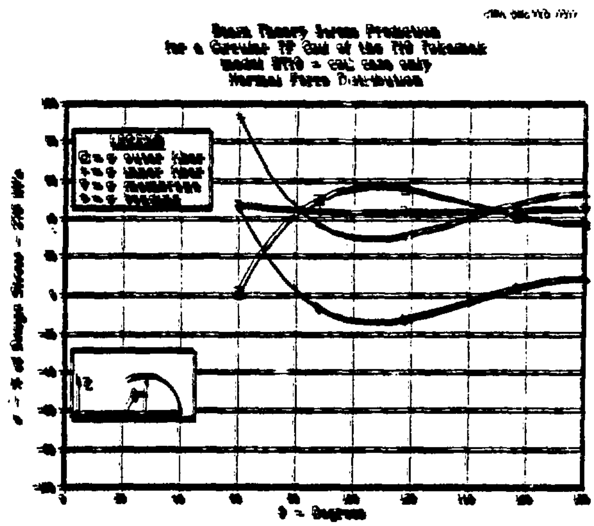

Figure 7.

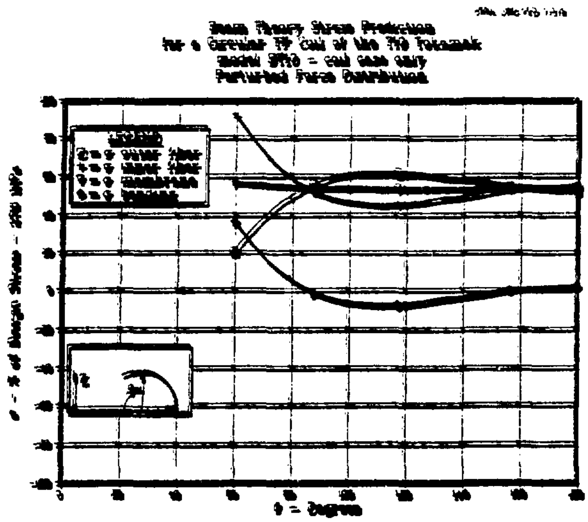

Figure 8.

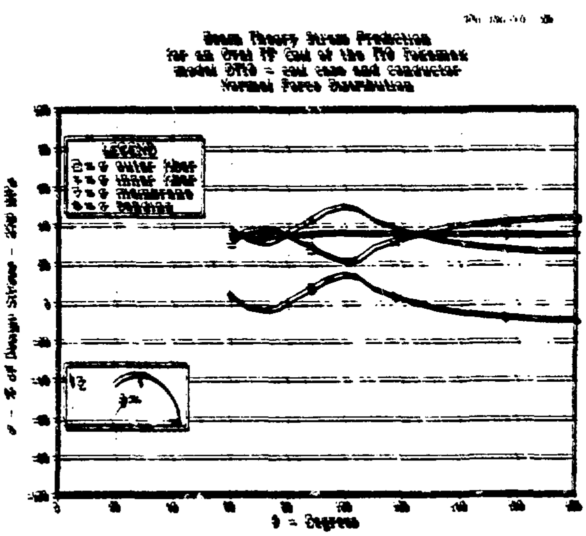

Figure 9.

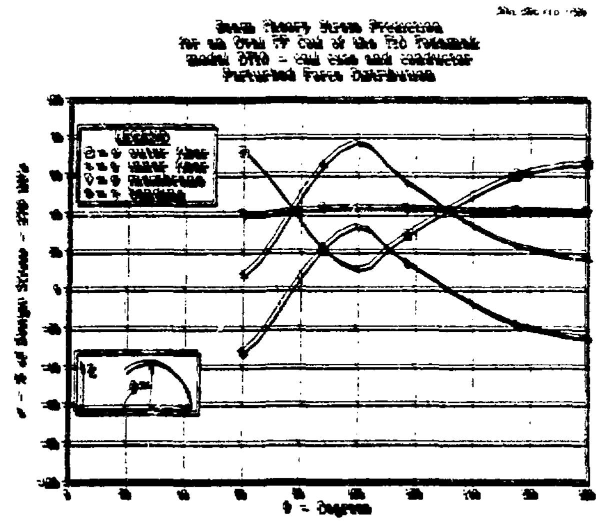

Figure 10.

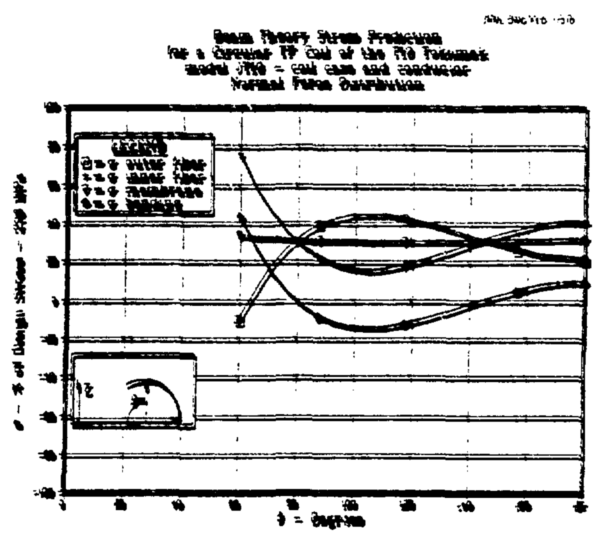

Figure 11.

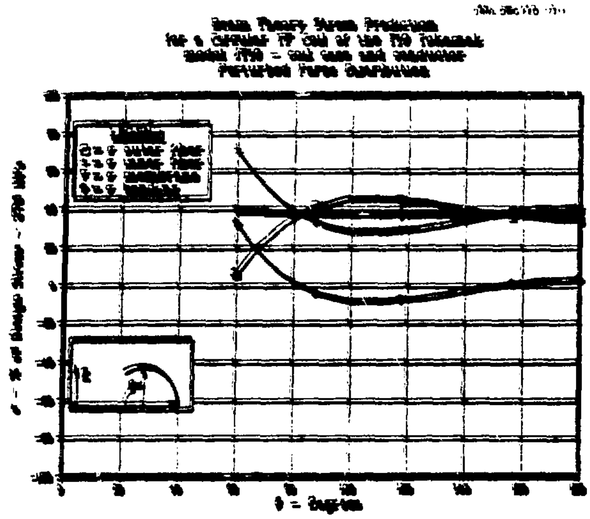

Figure 12.